Journal of Visualized Experiments

Standardized Histomorphometric Evaluation of Osteoarthritis in a Surgical Mouse Model

--Manuscript Draft--

Article Type:	Invited Methods Article - JoVE Produced Video
Manuscript Number:	JoVE60991R2
Full Title:	Standardized Histomorphometric Evaluation of Osteoarthritis in a Surgical Mouse Model
Section/Category:	JoVE Medicine
Keywords:	Osteoarthritis, DMM (Destabilization of Medial Meniscus), cartilage degeneration, joint pathology, quantitative evaluation, Histomorphometry
Corresponding Author:	Fadia Kamal, Ph.D. UNITED STATES
Corresponding Author's Institution:	
Corresponding Author E-Mail:	fkamal@pennstatehealth.psu.edu
Order of Authors:	William J. Pinamont
	Gregory M. Young
	Vengadeshprabhu Karuppagounder
	Natalie K. Yoshioka
	Elijah L. Carlson
	Adeel Ahmed
	Reyad Elbarbary
	Fadia Kamal, Ph.D.
Additional Information:	
Question	**Response**
Please indicate whether this article will be Standard Access or Open Access.	Standard Access (US$2,400)
Please indicate the **city, state/province, and country** where this article will be **filmed**. Please do not use abbreviations.	Hershey, Pa, USA

Cover Letter

PennState Health

MUSCULOSKELETAL SCIENCES
Mail Code H089
500 University Drive
Hershey, PA 17033
717-531-4819
717-531-0349 Fax

Orthopaedics and Rehabilitation

Dear Dr. Bajaj,

01/16/2020

Enclosed please find our second revision for our manuscript entitled “Standardized Histomorphometric Evaluation of Osteoarthritis in a Surgical Mouse Model”.

We thank the editor for their thorough review and insightful comments. Please find attached herewith the revised manuscript with all the comments and critiques addressed.

The protocol described in this manuscript uses the computerized and semi-automated OsteoMeasure system to establish a standardized, rigorous, and reproducible quantitative methodology for the evaluation of changes in cartilage and other joint components in osteoarthritis. This protocol presents a powerful addition to the existing systems, and allows for more efficient detection of changes in osteoarthritis.

We have highlighted the part to be scripted for videography. Please note that the script will focus on histomorphometry and not all the previous steps, since all the previous steps: mouse sacrifice, tissue processing and embedding, sectioning and staining, have been previously described in details, with some being available as *JoVe* videos.

In summary, the protocol detailed here provides a clear guide for a rigorous and reproducible computerized and semi-automated quantitative approach to investigate OA pathology or evaluate therapeutic interventions.

We sincerely hope you find our manuscript of interest to the audience of *JoVe*.

Best regards,

Fadia Kamal, PharmD, Msc, PhD
Assistant Professor
Department of Orthopedics and Rehabilitation
Penn State University, College of Medicine
500 University Drive
Room C3804C
Hershey, PA 17033-0850
ph 717-531-4808

TITLE:

Standardized Histomorphometric Evaluation of Osteoarthritis in a Surgical Mouse Model

AUTHORS AND AFFILIATIONS:

William J. Pinamont[1], Gregory M. Young[1], Vengadeshprabhu Karuppagounder[1], Natalie K. Yoshioka[1], Elijah L. Carlson[1], Adeel Ahmad[1], Reyad Elbarbary[1,2], Fadia Kamal[1,3*]

[1]Center for Orthopedic Research and Translational Sciences, Department of Orthopedics and Rehabilitation, Pennsylvania State College of Medicine, Hershey, Pennsylvania, USA
[2]Department of Biochemistry and Molecular Biology, Pennsylvania State College of Medicine, Hershey, Pennsylvania, USA
[3]Department of Pharmacology, Pennsylvania State College of Medicine, Hershey, Pennsylvania, USA

Corresponding Author:

Fadia Kamal (fkamal@pennstatehealth.psu.edu)

E-mail Addresses of Co-authors:

William Pinamont (wpinamont@pennstatehealth.psu.edu)
Greg Young (gregm.young1@gmail.com)
Vengadeshprabhu Karuppagounder (vkaruppagounder@pennstatehealth.psu.edu)
Natalie Yoshioka (nyoshioka@pennstatehealth.psu.edu)
Elijah Carlson (elc81@case.edu)
Adeel Ahmad (aahmad3@pennstatehealth.psu.edu)
Reyad Elbarbary (relbarbary@pennstatehealth.psu.edu)

KEYWORDS:

osteoarthritis, DMM, destabilization of medial meniscus, cartilage degeneration, joint pathology, quantitative evaluation, histomorphometry

SUMMARY:

The current protocol establishes a rigorous and reproducible method for quantification of morphological joint changes that accompany osteoarthritis. Application of this protocol can be valuable in monitoring disease progression and evaluating therapeutic interventions in osteoarthritis.

ABSTRACT:

One of the most prevalent joint disorders in the United States, osteoarthritis (OA) is characterized by progressive degeneration of articular cartilage, primarily in the hip and knee joints, which results in significant impacts on patient mobility and quality of life. To date, there are no existing curative therapies for OA able to slow down or inhibit cartilage degeneration. Presently, there is an extensive body of ongoing research to understand OA pathology and discover novel therapeutic approaches or agents that can efficiently slow down, stop, or even reverse OA. Thus, it is crucial to have a quantitative and reproducible approach to accurately evaluate OA-

associated pathological changes in the joint cartilage, synovium, and subchondral bone. Currently, OA severity and progression are primarily assessed using the Osteoarthritis Research Society International (OARSI) or Mankin scoring systems. In spite of the importance of these scoring systems, they are semiquantitative and can be influenced by user subjectivity. More importantly, they fail to accurately evaluate subtle, yet important, changes in the cartilage during the early disease states or early treatment phases. The protocol we describe here uses a computerized and semiautomated histomorphometric software system to establish a standardized, rigorous, and reproducible quantitative methodology for the evaluation of joint changes in OA. This protocol presents a powerful addition to the existing systems and allows for more efficient detection of pathological changes in the joint.

INTRODUCTION:

One of the most prevalent joint disorders in the United States, OA is characterized by progressive degeneration of articular cartilage, primarily in the hip and knee joints, which results in significant impacts on patient mobility and quality of life[1-3]. Articular cartilage is the specialized connective tissue of diarthrodial joints designed to minimize friction, facilitate movement, and endure joint compression[4]. Articular cartilage is composed of two primary components: chondrocytes and extracellular matrix. Chondrocytes are specialized, metabolically active cells that play a primary role in the development, maintenance, and repair of the extracellular matrix[4]. Chondrocyte hypertrophy (CH) is one of the principal pathological signs of OA development. It is characterized by increased cellular size, decreased proteoglycan production, and increased production of cartilage matrix-degrading enzymes that eventually lead to cartilage degeneration[5-7]. Further, pathological changes in the subchondral bone and synovium of the joint play an important role in OA development and progression[8-12]. To date, there are no existing curative therapies that inhibit cartilage degeneration[1-3,13,14]. Thus, there is extensive ongoing research that aims to understand OA pathology and discover novel therapeutic approaches that are able to slow down or even stop OA. Accordingly, there is an increasing need for a quantitative and reproducible approach that enables accurate evaluation of OA-associated pathological changes in the cartilage, synovium, and subchondral bone of the joint.

Currently, OA severity and progression are primarily assessed using the OARSI or Mankin scoring systems[15]. However, these scoring systems are only semiquantitative and can be influenced by user subjectivity. More importantly, they fail to accurately evaluate subtle changes that occur in the joint during disease or in response to genetic manipulation or a therapeutic intervention. There are sporadic reports in the literature describing histomorphometric analyses of the cartilage, synovium, or subchondral bone[16-21]. However, a detailed protocol for rigorous and reproducible histomorphometric analysis of all these joint components is still lacking, creating an unmet need in the field.

To study pathological changes in OA using histomorphometric analysis, we used a surgical OA mouse model to induce OA via destabilization of the medial meniscus (DMM). Among the established models of murine OA, DMM was selected for our study because it involves a less traumatic mechanism of injury[22-26]. In comparison to meniscal-ligamentous injury (MLI) or anterior cruciate ligament injury (ACLI) surgeries, DMM promotes a more gradual progression of

OA, similar to OA development in humans[22,24-26]. Mice were euthanized twelve weeks after DMM surgery to evaluate changes in the articular cartilage, subchondral bone, and synovium.

The goal of this protocol is to establish a standardized, rigorous, and quantitative approach to evaluate joint changes that accompany OA.

PROTOCOL:

Twelve-week-old male C57BL/6 mice were purchased from Jax Labs. All mice were housed in groups of 3–5 mice per micro-isolator cage in a room with a 12 h light/dark schedule. All animal procedures were performed according to the National Institute of Health (NIH) *Guide for the Care and Use of Laboratory Animals* and approved by the Animal Care and Use Committee of Pennsylvania State University.

1. Post-traumatic osteoarthritis (PTOA) surgical model

1.1. Anesthetize mice using a ketamine (100 mg/kg)/xylazine (10 mg/kg) combination via intraperitoneal injection, administer buprenorphine (1 mg/kg) via intraperitoneal injection for pain relief, and shave the hair over the knee. Check for the lack of a pedal reflex before starting the surgery.

1.2. Perform destabilization of the medial meniscus (DMM) surgery as previously described[22,23].

NOTE: Please refer to Glasson et al. and Singh et al. references for more detailed surgical protocol information[22,23].

1.2.1. Make a 3 mm longitudinal incision from the distal patella to the proximal tibial plateau of the right knee joint. Use a suture to displace the patellar tendon.

1.2.2. Open the joint capsule medial to the tendon and move the infrapatellar fat pad to visualize the intercondylar region, medial meniscus, and meniscotibial ligament[23].

1.2.3. Transect the medial meniscotibial ligament to complete DMM and destabilize the joint[22,23]. Close the incision site with staples or sutures.

1.3. Perform sham surgeries following a similar procedure, but without transection of the medial meniscotibial ligament.

NOTE: Mice were randomized to receive either DMM or sham surgery. According to the previously published literature, mice develop significant PTOA 12 weeks after the DMM surgery[22-24] .

2. Mouse euthanasia and sample collection

2.1. Mouse euthanasia

2.1.1. Twelve weeks after DMM, anesthetize mice using a ketamine (100 mg/kg)/xylazine (10 mg/kg) combination via intraperitoneal injection.

2.1.2. Make a midline incision through the skin along the thorax and retract the rib cage to expose the heart for perfusion fixation[27].

NOTE: Refer to the Gage et al. reference for additional information on the protocol for proper rodent fixation as well as the video depiction of the proper equipment assembly and procedures[27].

2.1.3. Set up the perfusion apparatus according to the manufacturer's protocol.

2.1.4. Euthanize the mouse by perfusing heparinized saline through the left ventricle until blood is cleared out and the liver becomes pale. Perfuse the mouse with 10% neutral buffered formalin until complete mouse fixation is achieved.

NOTE: A successfully perfused mouse will become stiff. The average perfusion time using the automated pump system is 5–7 min.

2.2. Sample collection and preparation

2.2.1. Isolate the knees by cutting the bone at mid-femur and mid-tibia and dissect the surrounding muscle tissue.

2.2.2. Continue the fixation by storing knee joints in 10% neutral buffered formalin at room temperature for 24 h, then at 4 ˚C for 6 days.

2.2.3. Decalcify the bone by storing the sample in EDTA decalcification buffer for 1 week at room temperature with mild shaking[28]. Change the decalcification buffer solution every 3 days.

NOTE: Decalcification buffer was prepared by dissolving 140 g of ultrapure EDTA tetrasodium in a solution of 850 mL of distilled water plus 15 mL of glacial acetic acid. The buffer was pH equilibrated to 7.6 by dropwise addition of glacial acetic acid to the solution. Upon reaching pH = 7.6, the buffer was brought to 1 L total volume with distilled water. Decalcification buffer was prepared fresh and used within 1 week of preparation.

2.2.4. Wash the knees with 50% ethanol, then 70% ethanol for 15 min each, then process for embedding.

NOTE: Fluid transfer processing was performed by the Molecular and Histopathology Core at Penn State Milton S. Hershey Medical Center. Consult the institution's histology core for recommendations on optimal sample processing.

2.2.5 Embed the mouse knees in paraffin with the medial aspect of the joint facing the bottom surface of the paraffin block. Apply slight pressure to the tibial side of the joint during embedding to ensure tibial and femoral surfaces are as close to the same plane as possible.

3. Microtome sectioning and slide selection

3.1. Microtome sectioning

3.1.1. Use the plane adjustment knobs on the block holder of the microtome to ensure proper facing of the sample block.

3.1.2. Face the paraffin block so that the distal aspect of the femur, proximal region of the tibia, and anterior and posterior horns of the medial meniscus appear in the same plane for section collection (**Supplementary Figure 1A**). Begin collecting sections on slides when the anterior and posterior horns of the medial meniscus begin to separate from one another.

3.1.3. Ensure that the tibia, femur, and menisci appear in same plane by comparing structure sizes. The tibia and femur should be of comparable size, with both meniscal horns similar in size and shape (**Supplementary Figure 1A**). If a structure appears too large in comparison to its counterpart, this indicates that additional facing is needed. Importantly, confirm that the joint space remains intact.

3.1.4. Take sagittal sections of the paraffin-embedded mouse knees through the medial joint compartment in 5 μm sections and collect the sections on slides. Collect approximately 30 sections per paraffin block.

3.2. Slide selection

3.2.1. Select three representative sections 50 μm apart for each sample starting from the fifth section (i.e., slides 5, 15, and 25). Selected slides will be used for subsequent staining, OARSI scoring, and histomorphometric analysis.

NOTE: From a block with 30 total sections, select slides from the beginning (slides 5–10), middle (slides 15–20), and end (slides 25–30) of the set in order to clearly represent the entire sample. Select slides from similar levels of depth between samples.

4. Hematoxylin, Safranin Orange, and Fast Green staining

4.1. Deparaffinize the selected slides with three changes of xylene. Hydrate the slides with two changes of 100% ethanol, two changes of 95% ethanol, and one change of 70% ethanol.

4.2. Stain the slides with hematoxylin for 7 min then wash with running water for 10 min. Stain with Fast Green for 3 min and rinse in 1.0% glacial acetic acid for 10 s. Stain with Safranin-O for 5

min and quickly rinse by dipping in 0.5% glacial acetic acid.

4.3. Rinse slides in two changes of distilled water and let air dry.

4.4. Clear slides in three changes of xylene for 5 min each then mount with xylene-based mounting media and a coverslip.

NOTE: Hematoxylin serves as the nuclear stain for identifying areas of bone marrow. Safranin-O is used to stain cartilage, proteoglycans, mucin, and mast cell granules. Fast Green is used as a counterstain for bone.

5. Slide imaging

5.1. Image the Safranin-O and Fast Green stained slides using an available camera attached to a microscope and computer-based imaging software.

5.2. Open the imaging software (see **Table of Materials**) and arrange the knee joint region of interest (ROI) in the center of the imaging window. If using a rotational microscope slide stage, align the slide so that the tibial surface spans the width of the horizontal axis of the imaging region.

5.3. Set the white balance of the camera before beginning to image a set of samples (**Supplementary Figure 2**). Image the joint compartment at both 4x and 10x magnification, ensuring that both the tibial and femoral articular surface and tibial subchondral bone are included within each of the image ROIs (**Supplementary Figure 1A**, **B**). Save images for each of the three selected levels to be used for OARSI scoring.

NOTE: Setting the white balance of the camera will depend on the software and camera systems being used. Generally, navigate to the **Camera Tab** or **Main Imaging Menu** and scroll down to **Set White Balance**. Select **Set White Balance** and a small cursor or icon should appear (**Supplementary Figure 2A**). Using the cursor, select an area within the image/sample that is free of stain, such as the joint space, to set the white balance.

6. Osteoarthritis research society international (OARSI) scoring[15]

6.1. Randomize the three selected Safranin-O and Fast Green stained slides from all samples.

6.2. Perform OARSI scoring in a blinded manner with three observers. Briefly, display one image at a time in a randomized order and allow three observers to score each image, correlating to one of the three levels selected for each sample.

NOTE: Please refer to the OARSI scoring table for detailed descriptions of the grading scale[15].

6.3. Calculate the average score for each section using individual scores from each observer.

Determine the average score per sample by taking the average score of the three representative sections.

7. Histomorphometric analysis

NOTE: Live images of the knee joint are viewed on a touchscreen monitor using a microscope camera, and a stylus is used to manually trace the ROIs. Built-in algorithms of the histomorphometry software quantify the specified parameters (see Protocol below) in the defined ROIs. Importantly, the same Safranin-O and Fast Green stained sections used in OARSI scoring are used for histomorphometric analysis.

7.1. Software setup and measurement preparation

7.1.1. Turn on microscope, camera, computer, and touchscreen monitor. Click on the **Software Icon** to launch the software program. Place the slide on the microscope stage for viewing.

7.1.2. Center the sample within the measurement window. Ensure that the measurement grid is set to the proper magnification to match the objective being used on the microscope (**Supplementary Figure 3**).

7.1.3. Go to the **File** tab at the top of the screen and scroll down to **Read Settings**. Open the **Settings** window and select the appropriate settings file for the parameters to be measured.

7.1.4. Select the parameter to be measured from the list on the right hand side of the screen (**Supplementary Figure 3**). Use the stylus or mouse cursor to trace images according to steps described below in order to measure specific tissue ROIs. When completed with each measurement, **Right Click** to end the measurement and continue to the next parameter.

NOTE: The list of parameters to be measured is created through a distinct preference file that is set up in consultation with the software company for the purpose of measuring the described ROIs. Please see discussion for further details regarding the complete setup.

7.1.5. Complete all measurements and then navigate to the **Summary Data** tab at the bottom of the software screen (**Supplementary Figure 3**). Click on the screen window, hit the **Insert** key on the keyboard or copy and paste the data into a separate spreadsheet.

NOTE: Perform histomorphometric analysis in a randomized and blinded manner. After completing all parameter measurements for all samples, organize the data and average the measurements from the three slides from each sample.

7.2. Measurements of the total, calcified, and uncalcified cartilage areas

NOTE: Use a commercially available software (see **Table of Materials**) to perform these steps. Please see **Supplementary Figure 1B**,**C** for clarification on cartilage regions, junctions, and subchondral bone regions discussed throughout this section.

7.2.1. Draw a line across the superior edge of the tibial cartilage surface where the cartilage meets the joint space. Draw a second line at the chondro-osseous junction where the calcified cartilage meets the subchondral bone (**Figure 1B**). Use the software **Area** function to automatically obtain the total cartilage area measurement.

7.2.2. Draw a line along the tidemark, a naturally occurring line separating the calcified and uncalcified regions of cartilage. Draw a second line at the chondro-osseous junction where the calcified cartilage meets the subchondral bone (**Figure 1B**). Use the software **Area** function to automatically obtain the calcified cartilage area measurement.

7.2.3. Calculate the uncalcified cartilage area by subtracting the calcified cartilage area from the total cartilage area (**Figure 1B**).

7.3. Determination of the chondrocyte number and phenotype

7.3.1. Create separate count functions within the settings in the histomorphometry software to distinguish matrix producing and matrix nonproducing chondrocytes (**Figure 1B**).

7.3.2. Determine the number of matrices producing or not producing chondrocytes by using the stylus to make a small dot over each chondrocyte expressing the specified phenotype (**Figure 1B**).

NOTE: Count cells according to their phenotype as either matrix producing (i.e., strong Safranin-O staining) or matrix nonproducing (i.e., very faint or no Safranin-O staining).

7.4. Measurement of the tibial articular surface perimeter

7.4.1. Measure the absolute tibial articular surface perimeter by tracing a line across the surface of the tibial cartilage, carefully defining individual fibrillations (**Figure 1C**).

7.4.2. Draw a second line along the tidemark to serve as an internal control for the plane of each section (**Figure 1C**).

7.4.3. Calculate the tibial articular surface fibrillation index by dividing the tibial articular surface perimeter by the tidemark perimeter.

NOTE: Tidemark perimeters are generally equal across samples, so the difference in the articular surface perimeters between sham and DMM was generally small whether absolute perimeter or fibrillation index were used.

7.5. Measurement of the subchondral bone and marrow space areas

7.5.1. Measure the subchondral marrow space area using the **Area** function by outlining regions in the subchondral region stained with hematoxylin only (i.e., negative for Fast Green) to determine total marrow space area within the subchondral bone. Draw lines around the perimeter of these areas to determine the total area of all marrow space within the tibial subchondral bone (**Figure 2B**).

7.5.2. Measure the total subchondral area using the area function by outlining the region between the chondro-osseous junction and the superior border of the growth plate, extending laterally to the regions of the anterior and posterior osteophytes (**Figure 2B**).

7.5.3. Calculate the subchondral bone area by subtracting the subchondral bone marrow space area from the total subchondral area (**Figure 2B**,**C**).

7.6. Measurement of the anterior and posterior osteophyte areas

7.6.1. To measure the osteophyte area, trace the anterior and posterior osteophytes of the proximal tibia using the **Area** function (**Figure 2B**,**E**,**F**).

NOTE: Osteophytes are bony projections that form between the articular cartilage and the growth plate, anterior or posterior to the subchondral region. Osteophyte areas on the anterior and posterior sides of the tibia are determined by tracing the area anterior or posterior to the subchondral bone. The junction between the osteophytes and subchondral bone is clearly delineated by a line of cells extending from the articular cartilage to the growth plate. The junction between the osteophyte and synovium is defined by a transition between bony and fibrous tissue.

7.7. Measurement of the synovial thickness

7.7.1. Measure the anterior femoral synovial thickness using the **Area** function by drawing a line from the inner insertion point of the anterior synovium on the femur towards its attachment point on the meniscus (**Figure 3B**).

7.7.2. Draw a second line from the outer insertion of the synovium on the femur towards its attachment to the meniscus (**Figure 3B**).

7.7.3. Calculate the synovial thickness by dividing the total synovial area by the synovial perimeter.

8. Statistical analysis

8.1. Collect the measured parameters and average the results from the three representative sections for each sample. Analyze the data using an unpaired Student's t-test to compare two groups or one-way ANOVA to compare three or more groups.

8.2. Display the data as mean ± standard error of mean.

NOTE: Statistical significance was achieved at $p \leq 0.05$.

REPRESENTATIVE RESULTS:

DMM-induced OA results in articular cartilage degeneration and chondrocyte loss

DMM-induced OA resulted in an increased OARSI score compared to sham mice, distinctly characterized by surface erosion and cartilage loss (**Figure 1A**,**D**). The histomorphometry protocol detailed here detected several OA-associated changes, including a decrease in total cartilage area and in the uncalcified cartilage area (**Figure 1A**,**B**,**E**,**G**); reduction in the total chondrocyte number; and, importantly, loss of matrix producing chondrocytes (**Figure 1H**,**I**). Changes to the articular surface, indicative of the severity of erosion, were evaluated using the cartilage fibrillation index. Overall, the fibrillation index increased in DMM mice (**Figure 1C**,**K**,**L**). However, it is also important to note that the fibrillation index may decrease in end-stage OA due to complete erosion of the cartilage surface, as discussed in the Protocol. An increase in the fibrillation index signifies degeneration of the articular cartilage surface during OA development and progression. These results highlight the ability of the histomorphometric analysis program to detect and quantify pathological cartilage changes that characterize OA progression.

Assessment of other joint changes in DMM-induced OA

OA affects joint tissues other than the cartilage, and pathological changes in these tissues play a crucial role in disease progression. Here, the described histomorphometric analysis method revealed an increase in the subchondral bone area and a reduction in the area of the bone marrow space in DMM mice (**Figure 2A**–**D**), indicating subchondral bone sclerosis[29,30]. Both anterior and posterior osteophyte areas also increased in DMM mice (**Figure 2E**,**F**), suggesting an ongoing subchondral bone remodeling that acts as a compensatory mechanism to handle changes in joint loading at the site of injury[29,30].

Histomorphometric analysis of the synovium showed increased synovial thickness in DMM mice (**Figure 3A**–**C**), which is a typical outcome of OA-associated synovial inflammation and the diffusion of inflammatory cytokines into the joint space[11,12,31-34].

Analysis of interuser variability between OARSI scoring versus histomorphometry

Figure 4A shows no significant interuser variability of both histomorphometric analysis of the uncalcified cartilage area (**Figure 4A**) and the OARSI score (**Figure 4B**). However, the histomorphometric analysis showed an extremely low mean difference in between observers ranging from -0.0001179–0.00120, leading to an almost complete overlap of the results obtained by the three observers, while the mean difference between observers was higher in the OARSI score ranging from -0.3–0.3 with a clear deviation of O1 values from O2 and O3 values.

FIGURE LEGENDS:

Figure 1: Histomorphometry of tibial articular cartilage and articular chondrocyte phenotypes from sham surgery and DMM mice. (**A**) Tibial articular surface stained with Safranin-O/Fast

Green. (**B**) Histomorphometric analysis was used to trace the total cartilage area and the calcified cartilage area (orange). The cartilage superior to the tidemark area was calculated as the uncalcified cartilage (green). Matrix producing chondrocytes (white) and matrix nonproducing chondrocytes (magenta) were counted within the uncalcified cartilage area. (**C**) The tibial articular surface perimeter was measured by tracing the articular surface (blue line) followed by the tidemark (purple line) to determine the fibrillation index. (**D**) The OARSI score increased in DMM mice. (**E–L**) Graphical representation of the quantified cartilage areas and chondrocyte counts from sham and DMM mice. Compared to sham mice, DMM mice had decreased total tibial cartilage area (**E**), tibial calcified cartilage area (**F**), tibial uncalcified cartilage (**G**), tibial total chondrocyte number (**H**), tibial matrix producing chondrocytes, (**I**) and tibial matrix nonproducing chondrocytes (**J**). Compared to sham mice, DMM mice had increased tibial articular surface perimeter (**K**) and increased tibial articular surface fibrillation index (**L**). Images were taken using 10x magnification. *$P < 0.05$, **$P < 0.01$, ***$P < 0.001$, and ****$P < 0.0001$ using unpaired t-test with Welch's correction, values are expressed as mean $\pm$ SEM; n = 5/group.

Figure 2: Histomorphometry of subchondral bone marrow area and subchondral bone area from sham surgery and DMM mice. (**A**) Tibial articular cartilage and subchondral bone stained with Safranin-O/Fast Green. (**B**) The subchondral bone marrow areas (green), subchondral bone area (magenta), anterior osteophyte area (yellow), and posterior osteophyte area (gray) were traced with computed histomorphometry software. (**C–F**) Graphed histomorphometric areas between the sham and DMM mice. Compared to the sham mice, DMM mice had an increased tibial subchondral bone area (**C**) and tibial anterior and posterior osteophyte areas (**E–F**), as well as decreased tibial subchondral bone marrow area compared to sham mice (**D**). Images were taken using 4x magnification. *$P < 0.05$, **$P < 0.01$ using unpaired t-test with Welch's correction. Values are expressed as mean $\pm$ SEM; n = 5/group.

Figure 3: Histomorphometry of synovium from sham surgery and DMM mice. (**A**) Synovium stained with Safranin-O/Fast Green. (**B**) The synovial thickness was measured by tracing the anterior meniscofemoral synovial membrane across the anterior aspect of the tibiofemoral joint (green). (**C**) Graphical representation of synovial thickness measurements using computed histomorphometry software. DMM mice had an increased synovial thickness compared to sham mice. Images were taken at 20x magnification. ***$P < 0.001$ using unpaired t-test with Welch's correction, values are expressed as mean $\pm$ SEM; n = 5/group; S = synovium; F = femur; and M = meniscus.

Figure 4. Interuser variability in OARSI scoring versus histomorphometric analysis. (**A**) Uncalcified cartilage area measurements obtained using histomorphometry by three blinded observers (O1, O2, O3). (**B**) OARSI scores for sham and DMM mice obtained from the three blinded observers. The dotted lines denote the mean value for each group.

Supplementary Figure 1: Histological analysis of Safranin-O and Fast Green stained mouse tibiofemoral joint sections. (**A**) A 4x magnification image of the tibiofemoral joint. Areas of focus are labeled. (**B**) A 10x magnification image of the tibiofemoral joint ROI. The tibial and femoral surfaces as well as the anterior and posterior meniscal horns are visualized. The menisci are

approximately the same size and the imaging ROI is centered on the joint compartment. (**C**) A 40x magnification image of the proximal tibial surface. The tidemark line is labeled as the line between the uncalcified and calcified cartilage zones. The osteochondral junction is labeled between the end of the calcified cartilage and beginning of the subchondral bone.

Supplementary Figure 2: Histomorphometry system setup and camera white balance calibration. (**A**) Mouse tibiofemoral joint visualized at 4x magnification in the software window with white balance not set. Note the camera settings tab at the top of the screen and the selection in the dropdown menu to set the white balance. (**B**) Mouse tibiofemoral joint at 4x magnification with white balance set. Note the change in the coloration and staining of the sample, increasing the user's ability to distinguish certain areas of the tibiofemoral joint when performing measurements.

Supplementary Figure 3: Setup of histomorphometric software prior to histomorphometric analysis measurements. Representative screenshot of the histomorphometric software window. Note the stained mouse knee section is centered in the measurement region (yellow grid) and the correct magnification scale for the region is selected to match the objective being used on the microscope (circled in red in the top right hand corner of the screen). The list of parameters is displayed in the column to the right of the imaging and measurement area. Selecting a parameter will highlight the parameter, hence **Tibial Fibrillation** is currently selected to be measured. The **Summary Data** tab at the bottom of the window is where measurements for each parameter for each sample will be organized and saved to be exported following completion of each parameter measurement for each section.

DISCUSSION:

Recent osteoarthritis research has enhanced our understanding of the crosstalk between the different tissues within the joint and the role each tissue plays in disease initiation or progression[8-10,35,36]. Accordingly, it has become obvious that the assessment of OA should not be limited to analysis of the cartilage but should also include analysis of the subchondral bone and synovium. In spite of that, the articular cartilage has been the primary focus of semiquantitative scoring of OA[15,37,38]. Although computed histomorphometry has already been applied to various areas of musculoskeletal research[39-44], there is an unmet gap in describing a protocol to accurately and reproducibly analyze discrete changes to the multitude of tissues within the knee joint compartment during OA. The application of histomorphometric analysis measurements to quantify changes to the cartilage, subchondral bone, and synovium provides a more holistic assessment of the primary and secondary changes in OA joints.

Here, we describe for the first time a detailed protocol that utilizes a computerized and semiautomated histomorphometric analysis software to quantify pathological changes in different joint compartments and evaluate OA development, progression, or regression. Care should be taken during sample preparation, as clear and consistent Safranin-O and Fast Green stains are essential to limit ambiguity when tracing and taking measurements with histomorphometric software. Using fresh staining solutions for each batch of slides is advisable. In addition, slide selection for staining must occur at consistent levels between blocks. The first

slide must be taken at a similar level between samples, ideally as soon as the anterior and posterior meniscal horns start separating.

During OA, total cartilage and uncalcified cartilage areas decrease due to cartilage fibrillation and degeneration. In severe OA, complete degeneration of the calcified cartilage may also occur. The protocol highlights the significance of determining the chondrocyte phenotype as an assessment of OA progression for the evaluation of anabolic versus catabolic signaling in cartilage. The total number of chondrocytes and the number of matrix producing chondrocytes (anabolic) are high in normal cartilage and low in OA cartilage, where the majority of existing chondrocytes in OA are matrix nonproducing (catabolic). Importantly, this essential parameter in the field of OA therapeutic discovery is not evaluated by OARSI or Mankin's scoring systems. Certain interventions that not only preserve the cartilage area and the number of chondrocytes but also promote chondrocyte anabolic phenotype may be more effective therapeutic approaches.

The protocol detailed here also provides a method to quantitatively measure the subtle changes in cartilage surface fibrillations present in mild to moderate OA. A greater number of fibrillations means an increased perimeter measurement due to the presence of indentations in the articular surface. Thus, the tibial articular surface perimeter and fibrillation index are low in normal cartilage, intermediate in mild OA due to some fibrillations, high in moderate OA due to more fibrillations, but again low in severe OA due to complete cartilage degeneration and loss.

Subchondral bone remodeling and sclerosis are characteristic pathological signs of OA, resulting in reduced subchondral marrow space area and increased subchondral bone area[8-10,29,30]. Quantification of changes in the subchondral bone area and subchondral marrow space area described in the protocol demonstrate the importance of understanding multi-tissue changes as a driving component for the complex nature of OA disease development and progression. Measurement of the anterior and posterior osteophyte areas provides important insight into the scale of bone remodeling occurring within the joint. The osteophyte area is extremely small in sham-operated knees and is increased due to osteophyte formation in OA. Measurement of the anterior osteophyte area differed slightly from the measurement of the posterior osteophyte area due to the severe nature of bone remodeling occurring at the medial region of the knee, near the site of DMM injury.

Finally, this protocol outlines a quantifiable assessment of changes in the synovial membrane. Synovial thickness is low in sham joints and increases in OA. Inflammation in OA leads to thickening of the synovial membrane to increase delivery of inflammatory cytokines and other factors to the joint space[10-12,31,32]. Thus, it is essential to evaluate joint inflammation as a modulating factor of OA disease progression.

Use of the histomorphometry software is limited by the availability of the hardware: touchscreen monitors or tablets with a stylus are absolutely necessary given the amount of manual tracing required for taking accurate measurements. Attempting to measure small areas with the histomorphometry software can also be limiting, as the pen size is restricted to one diameter. While this inability to measure small areas may be inconvenient, the joint areas measured are

easily defined with the area tool, and the low discrimination of the software makes a negligible difference in the final measurement.

It should also be noted that interuser variability is always an area of concern regarding implementation of a reliable and reproducible quantitative protocol. Establishing an effective, reproducible, and rigorous histomorphometry protocol requires limiting potential compounding variables within the experimental analysis, including reducing interuser variability. However, following a short training session (about 30 min) with the software, lab members were able to generate highly consistent and reproducible measurements, where the distribution of measurements between users reflects more of a direct overlay representing almost no interuser variability. Importantly, this histomorphometry protocol demonstrates an efficient method to quantify even discrete differences between sham samples in a highly reproducible manner.

The OARSI scoring system is a commonly used measure of assessment for cartilage damage in OA patients and experimental murine models[15]. The scoring system is based on a whole-number scale primarily focused on the extent of clefts/erosion or the articular surface. Although we found no significant interuser variability with the OARSI scores in our experiment, there still was a higher mean difference in between observers, versus almost none in the described histomorphometry protocol. Thus, establishing this reproducible protocol for histomorphometric analysis of defined parameters allows for highly consistent measurements of each sample, even between multiple users, removing some of the subjective nature of sample analysis.

The OARSI standardized scoring system is a benchmark for OA research. However, the limited score-based nature of the system does not allow for quantification of subtle changes occurring within the joint. The expanded joint evaluation described in this manuscript using histomorphometry software provides an enhanced and less subjective characterization of the severity of OA. This protocol is optimized for mice that have undergone a surgical induction of OA. The procedures and techniques can be applied for evaluation of OA within other models and hypotheses, however.

In summary, the protocol detailed here provides a clear guide for a rigorous and reproducible semiautomated quantitative approach to investigate OA pathology or evaluate therapeutic interventions.

ACKNOWLEDGMENTS:
We would like to acknowledge the assistance of the Department of Comparative Medicine staff and the Molecular and Histopathology core at Penn State Milton S. Hershey Medical Center. Funding sources: NIH NIAMS 1RO1AR071968-01A1 (F.K.), ANRF Arthritis Research Grant (F.K.).

DISCLOSURES:
None

REFERENCES:

1. Ma, V. Y., Chan, L., Carruthers, K. J. Incidence, prevalence, costs, and impact on disability of common conditions requiring rehabilitation in the United States: stroke, spinal cord injury, traumatic brain injury, multiple sclerosis, osteoarthritis, rheumatoid arthritis, limb loss, and back pain. *Archives of Physical Medicine and Rehabililation.* **95** (5), 986–995 (2014).
2. Hopman, W. et al. Associations between chronic disease, age and physical and mental health status. *Journal of Chronic Diseases in Canada.* **29** (3), 108–116 (2009).
3. Lorenz, J., Grässel, S. Experimental osteoarthritis models in mice. In *Mouse Genetics. Methods in Molecular Biology*. ed., Singh S., Coppola V., vol 1194, 401–419, Humana Press. New York, NY (2004).
4. Sophia Fox, A. J., Bedi, A., Rodeo, S. A. The basic science of articular cartilage: structure, composition, and function. *Journal of Sports Health.* **1** (6), 461–468 (2009).
5. Van der Kraan, P., Van den Berg, W. Chondrocyte hypertrophy and osteoarthritis: role in initiation and progression of cartilage degeneration? *Osteoarthritis and Cartilage.* **20** (3), 223–232, (2012).
6. Hodsman, A. B. et al. Parathyroid hormone and teriparatide for the treatment of osteoporosis: a review of the evidence and suggested guidelines for its use. *Endocrine Reviews.* **26** (5), 688–703 (2005).
7. Pitsillides, A. A., Beier, F. Cartilage biology in osteoarthritis—lessons from developmental biology. *Nature Reviews Rheumatology.* **7** (11), 654 (2011).
8. Yuan, X. et al. Bone–cartilage interface crosstalk in osteoarthritis: potential pathways and future therapeutic strategies. *Osteoarthritis and Cartilage.* **22** (8), 1077–1089 (2014).
9. Goldring, S. R., Goldring, M. B. Changes in the osteochondral unit during osteoarthritis: structure, function and cartilage–bone crosstalk. *Nature Reviews Rheumatology.* **12** (11), 632 (2016).
10. Martel-Pelletier, J. et al. Osteoarthritis. *Nature Reviews Disease Primers.* **2** (1), 16072 (2016).
11. Goldring, M. B., Otero, M. Inflammation in osteoarthritis. *Current Opinion in Rheumatology.* **23** (5), 471 (2011).
12. Sellam, J., Berenbaum, F. The role of synovitis in pathophysiology and clinical symptoms of osteoarthritis. *Nature Reviews Rheumatology.* **6** (11), 625 (2010).
13. Ma, H. et al. Osteoarthritis severity is sex dependent in a surgical mouse model. *Osteoarthritis and Cartilage.* **15** (6), 695–700 (2007).
14. Katon, W., Lin, E. H., Kroenke, K. The association of depression and anxiety with medical symptom burden in patients with chronic medical illness. *General Hospital Psychiatry.* **29** (2), 147–155 (2007).
15. Glasson, S., Chambers, M., Van Den Berg, W., Little, C. The OARSI histopathology initiative–recommendations for histological assessments of osteoarthritis in the mouse. *Osteoarthritis and Cartilage.* **18**, S17–S23 (2010).
16. Pastoureau, P., Leduc, S., Chomel, A., De Ceuninck, F. Quantitative assessment of articular cartilage and subchondral bone histology in the meniscectomized guinea pig model of osteoarthritis. *Osteoarthritis and Cartilage.* **11** (6), 412–423 (2003).
17. O'Driscoll, S. W., Marx, R. G., Fitzsimmons, J. S., Beaton, D. E. Method for automated cartilage histomorphometry. *Tissue Engineering.* **5** (1), 13–23 (1999).

18. Matsui, H., Shimizu, M., Tsuji, H. Cartilage and subchondral bone interaction in osteoarthrosis of human knee joint: a histological and histomorphometric study. *Microscopy Research Technique.* **37** (4), 333–342 (1997).
19. Hacker, S. A., Healey, R. M., Yoshioka, M., Coutts, R. D. A methodology for the quantitative assessment of articular cartilage histomorphometry. *Osteoarthritis and Cartilage.* **5** (5), 343–355 (1997).
20. Pastoureau, P., Chomel, A. Methods for Cartilage and Subchondral Bone Histomorphometry. In *Cartilage and Osteoarthritis. Methods in Molecular Medicine.* eds., De Ceuninck, F., Sabatini, M., Pastoureau, P., vol. 101, 79–91, Humana Press. New York, NY (2004).
21. McNulty, M. A. et al. A comprehensive histological assessment of osteoarthritis lesions in mice. *Cartilage.* **2** (4), 354–363 (2011).
22. Glasson, S., Blanchet, T., Morris, E. The surgical destabilization of the medial meniscus (DMM) model of osteoarthritis in the 129/SvEv mouse. *Osteoarthritis and Cartilage.* **15** (9), 1061–1069 (2007).
23. Singh, S. R., Coppola, V. *Mouse Genetics: Methods and Protocols*. Humana Press. New York, NY (2004).
24. Fang, H., Beier, F. Mouse models of osteoarthritis: modelling risk factors and assessing outcomes. *Nature Reviews Rheumatology.* **10** (7), 413 (2014).
25. Culley K. L. et al. Mouse Models of Osteoarthritis: Surgical Model of Posttraumatic Osteoarthritis Induced by Destabilization of the Medial Meniscus. In *Osteoporosis and Osteoarthritis*. *Methods in Molecular Biology*. eds., Westendorf J., van Wijnen A., vol. 1226, 143–173, Humana Press, New York, NY (2015).
26. Van der Kraan, P. Factors that influence outcome in experimental osteoarthritis. *Osteoarthritis and Cartilage.* **25** (3), 369–375 (2017).
27. Gage, G. J., Kipke, D. R., Shain, W. Whole animal perfusion fixation for rodents. *Journal of Visualized Experiments.* (65), e3564 (2012).
28. Callis, G., Sterchi, D. Decalcification of bone: literature review and practical study of various decalcifying agents. Methods, and their effects on bone histology. *Journal of Histotechnology.* **21** (1), 49–58 (1998).
29. Lajeunesse, D., Massicotte, F., Pelletier, J.-P., Martel-Pelletier, J. Subchondral bone sclerosis in osteoarthritis: not just an innocent bystander. *Modern Rheumatology.* **13** (1), 0007–0014 (2003).
30. Li, G. et al. Subchondral bone in osteoarthritis: insight into risk factors and microstructural changes. *Arthritis Research Therapy.* **15** (6), 223 (2013).
31. Kapoor, M., Martel-Pelletier, J., Lajeunesse, D., Pelletier, J.-P., Fahmi, H. Role of proinflammatory cytokines in the pathophysiology of osteoarthritis. *Nature Reviews Rheumatology.* **7** (1), 33 (2011).
32. Scanzello, C. R., Goldring, S. R. The role of synovitis in osteoarthritis pathogenesis. *Bone.* **51** (2), 249–257 (2012).
33. Benito, M. J., Veale, D. J., FitzGerald, O., van den Berg, W. B., Bresnihan, B. Synovial tissue inflammation in early and late osteoarthritis. *Annals of the Rheumatic Diseases.* **64** (9), 1263–1267 (2005).
34. De Lange-Brokaar, B. J. et al. Synovial inflammation, immune cells and their cytokines in osteoarthritis: a review. *Osteoarthritis and Cartilage.* **20** (12), 1484–1499 (2012).

35. Findlay, D. M., Kuliwaba, J. S. Bone–cartilage crosstalk: a conversation for understanding osteoarthritis. *Bone Research.* **4**, 16028 (2016).
36. Lories, R. J., Luyten, F. P. The bone–cartilage unit in osteoarthritis. *Nature Reviews Rheumatology.* **7** (1), 43 (2011).
37. Pritzker, K. P. et al. Osteoarthritis cartilage histopathology: grading and staging. *Journal of Osteoarthritis and Cartilage.* **14** (1), 13–29 (2006).
38. Hayami, T. et al. Characterization of articular cartilage and subchondral bone changes in the rat anterior cruciate ligament transection and meniscectomized models of osteoarthritis. *Bone.* **38** (2), 234–243 (2006).
39. Priemel, M. et al. Bone mineralization defects and vitamin D deficiency: Histomorphometric analysis of iliac crest bone biopsies and circulating 25-hydroxyvitamin D in 675 patients. *Journal of Bone and Mineral Research.* **25** (2), 305–312 (2010).
40. Yukata, K. et al. Continuous infusion of PTH 1–34 delayed fracture healing in mice. *Scientific Reports.* **8** (1), 13175 (2018).
41. Kawano, T. et al. LIM kinase 1 deficient mice have reduced bone mass. *Bone.* **52** (1), 70–82 (2013).
42. Zhang, L., Chang, M., Beck, C. A., Schwarz, E. M., Boyce, B. F. Analysis of new bone, cartilage, and fibrosis tissue in healing murine allografts using whole slide imaging and a new automated histomorphometric algorithm. *Bone Research.* **4**, 15037 (2016).
43. Wu, Q. et al. Induction of an osteoarthritis-like phenotype and degradation of phosphorylated Smad3 by Smurf2 in transgenic mice. *Arthritis Rheumatism.* **58** (10), 3132–3144 (2008).
44. Hordon, L. et al. Trabecular architecture in women and men of similar bone mass with and without vertebral fracture: I. Two-dimensional histology. *Bone.* **27** (2), 271–276 (2000).

Figure 1

Click here to access/download;Figure;Slide1.tiff

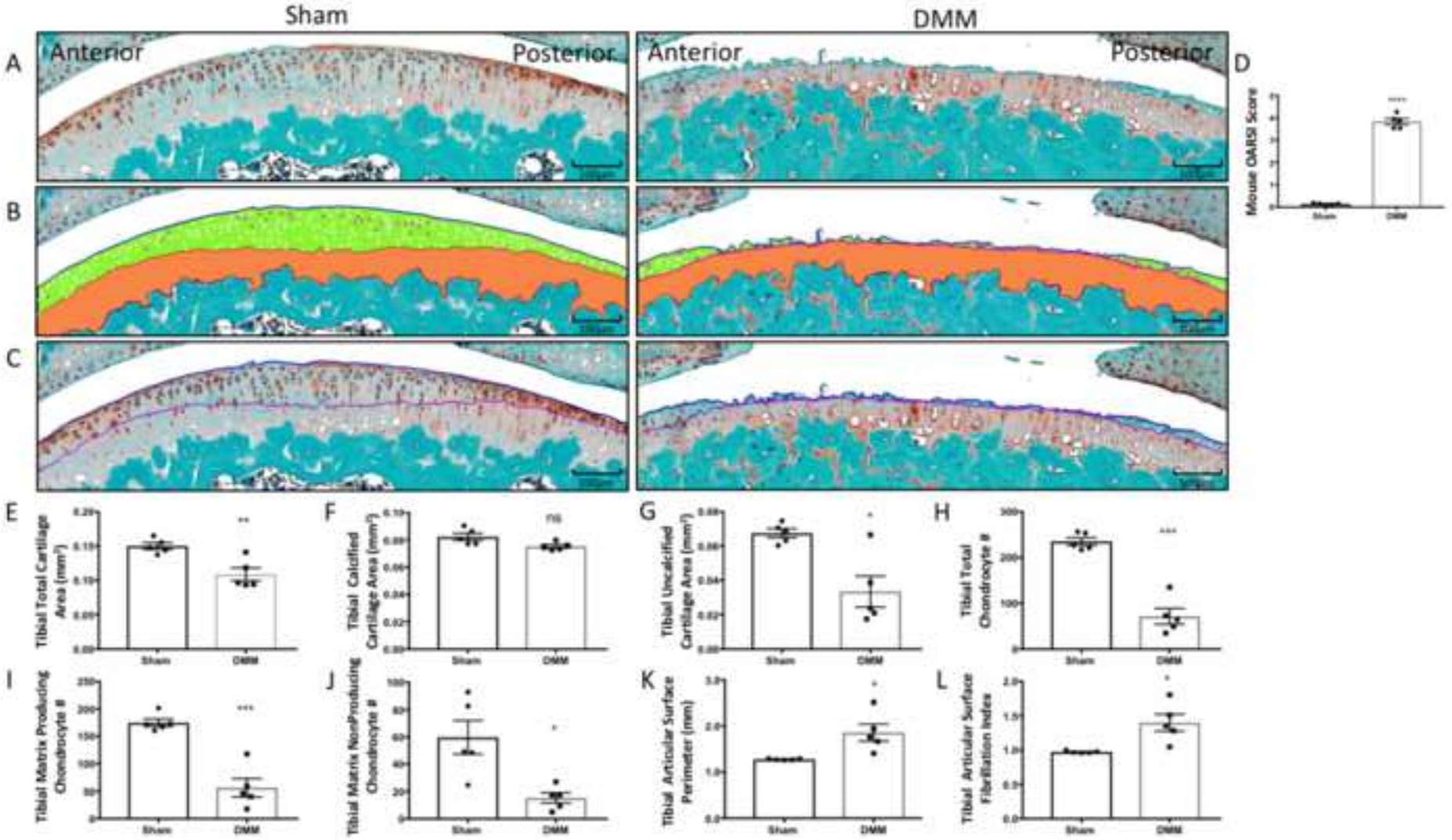

Figure 2

Click here to access/download;Figure;Slide2.tiff

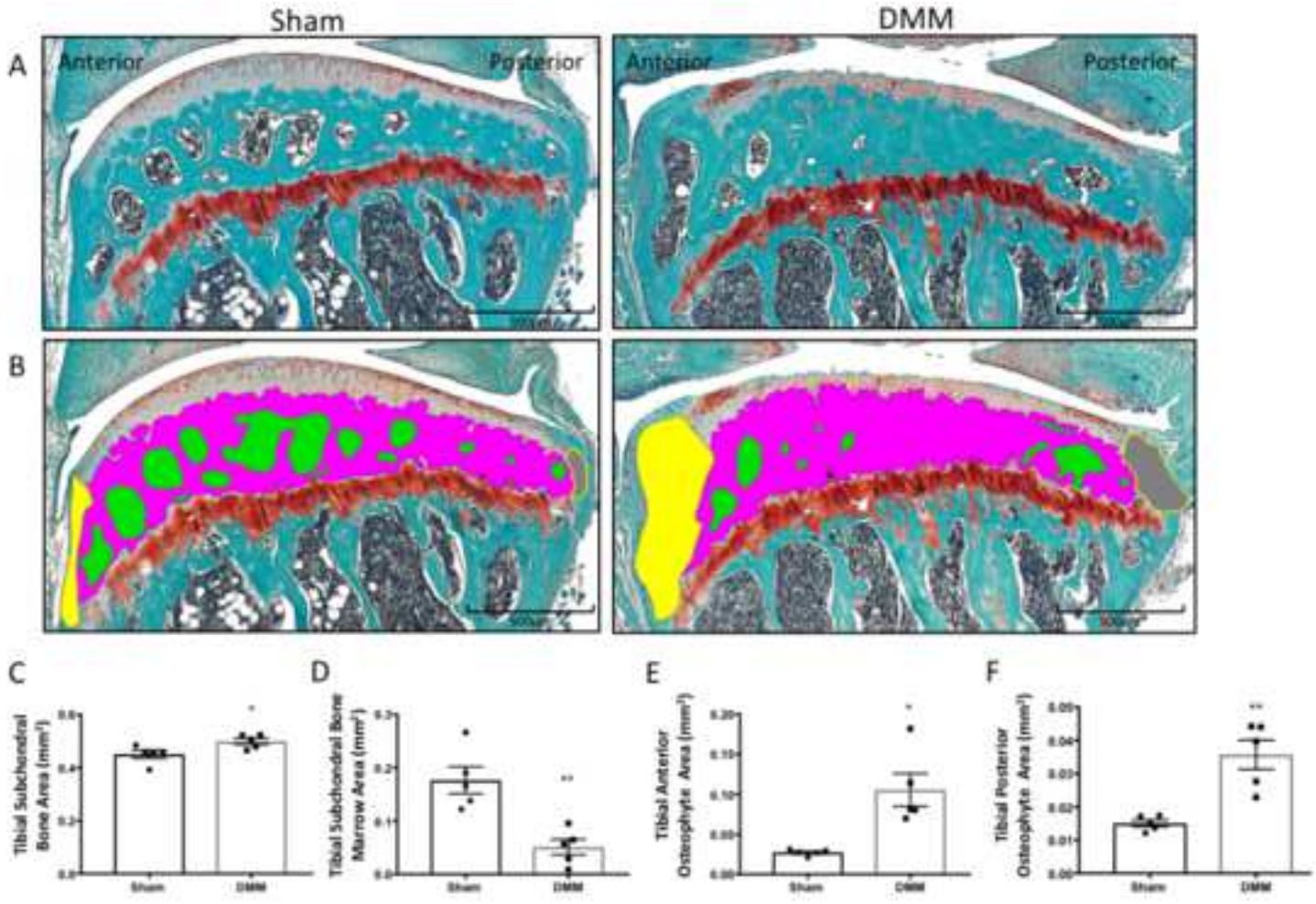

Figure 3

Click here to access/download;Figure;Slide3.tiff

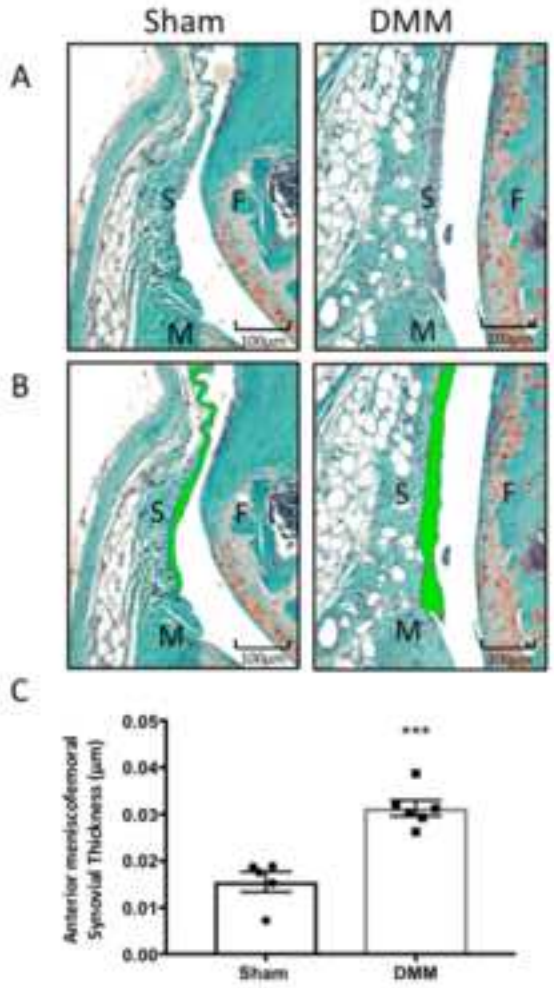

Figure 4

Click here to access/download;Figure;Slide4.tiff

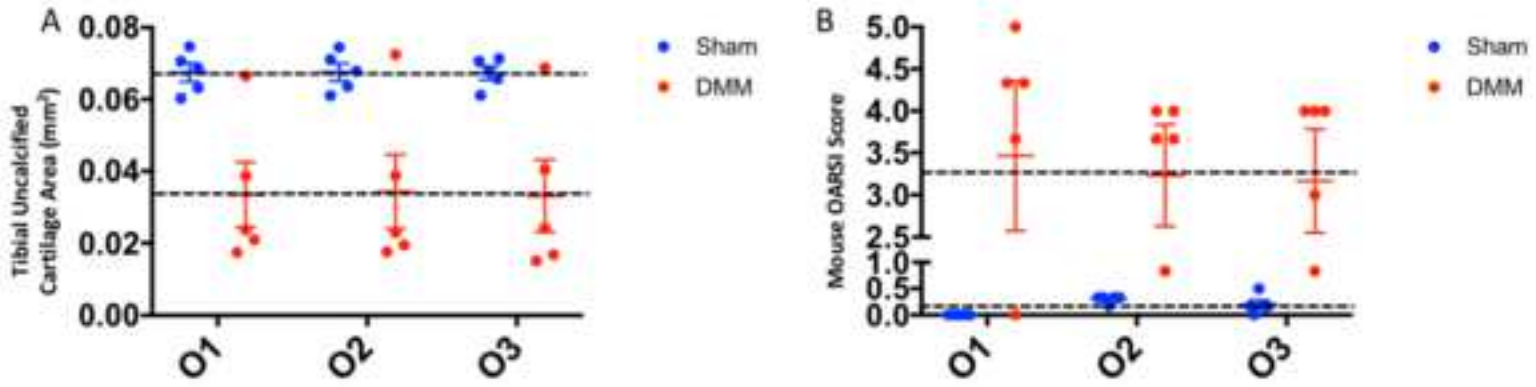

Table of Materials

Click here to access/download;Table of Materials;JoVE_Table_of_Materials R2.xlsx

Name of Material/Equipment	Company	Catalog Number
10% Buffered Formalin Phosphate	Fisher Chemical	SF100-20
Acetic Acid, Glacial (Certified A.C.S.)	Fisher Chemical	A38S-212
Cintiq 27QHD Creative Pen Display	Wacom	https://www.wacom.com/en-es/produ
Cintiq Ergo stand	Wacom	https://www.wacom.com/en-es/produ
Ethylenediaminetetraacetic acid, tetrasodium salt dihydrate, 99%	Acros Organics	AC446080010
Fast Green stain	SIGMA Life Sciences	F7258
Fisherbrand Superfrost Plus Microscope Slides	Fisher	12-550-15
HistoPrep Xylene	Fisherbrand	HC-700-1GAL
Histosette II Tissue Cassettes - Combination Lid and Base	Fisher	15-182-701A
HP Z440 Workstation	HP	Product number: Y5C77US#ABA
Manual Rotary Microtome	Leica	RM 2235
Marking pens	Leica	3801880
OLYMPUS BX53 Microscope	OLYMPUS	https://www.olympus-lifescience.com/
OLYMPUS DP 73 Microscope Camera	OLYMPUS	https://www.olympus-lifescience.com/
ORION STAR A211 pH meter	Thermo Scientific	STARA2110
OsteoMeasure Software	OsteoMetrics	https://www.osteometrics.com/index.
Perfusion Two Automated Pressure Perfusion system	Leica	Model # 39471005
PRISM 7 Software	GraphPad	Institutional Access Account
Safranin-O stain	SIGMA Life Sciences	S8884
ThinkBoneStage - Rotating Microscope Stage	Think Bone Consulting Inc. - OsteoMetrics (supplier)	http://thinkboneconsulting.com/index
Wacom Pro Pen Stylus	Wacom	https://www.wacom.com/en-es/produ
Weigerts Iron Hematoxylin A	Fisher	5029713
Weigerts Iron Hematoxylin B	Fisher	5029714

Comments/Description
For sample fixation following harvest
For Decalcification Buffer preparation and acetic acid solution preparation for staining
For histomorphometric analysis and imaging
For histomorphometric analysis and imaging
For Decalcification Buffer preparation
For sample staining
For sample section collection
For sample deparrafinization and staining
For sample processing and embedding
For histomorphometric analysis and imaging
For sample sectioning
For sample labeling, cassettes and slides
For histomorphometric analysis and imaging

or histomorphometric analysis and imaging (discontinued)

For Decalcification Buffer preparation
For histomorphometric measurement and analysis
For mouse knee harvest
Statistical Analysis
For sample staining
For histomorphometric analysis and imaging
For histomorphometric analysis and imaging
For hematoxylin staining
For hematoxylin staining

Response to JoVE editorial and peer review comment for: *A Standardized Approach to Histomorphometric Evaluation of Osteoarthritis in A Surgical Mouse Model*

First, we would like to thank the editor and reviewers for taking the time to review our work and provide us with their valuable comments. Below is a numerical list of the editor's comments addressed one at a time.

1. Document has been proofread and spelling and grammar issues have been addressed.
2. Email addresses have been provided for each author (lines 21-27).
3. Abbreviations missing definitions have been corrected, specifically OARSI on line 49 in the introduction section.
4. Commercial language has been removed throughout the protocol.
5. Animal ethics statement has been moved to the beginning of the Protocol section (lines 97-101).
6. Protocol has been modified to include action items with the intent of directing readers through the described protocol. Supplemental information originally included throughout the protocol section has been moved to the discussion section.
7. Protocol numbering format has been modified in accordance with JoVE instructions. Bullets and dashes have been removed throughout.
8. A single line space between each step, substep, and note has been included in the newly revised protocol section.
9. Protocol section has been modified to use the imperative tense and modified with more direct action words and steps to lead through the protocol.
10. Protocol has been simplified to more discrete action steps to direct readers through each distinct step within the protocol.
11. Previous significance subsections within the protocol sections have been moved to the discussion section.
12. "How" questions for each step were answered/addressed to the best of our ability without providing excessive extraneous details.
13. The volume and concentration of ketamine/xylazine drug combination was described in greater detail. We have also provided greater detail regarding secondary step for euthanasia by perfusion fixation. Detailed actions of knee joint harvesting and decalcification steps have been provided.
14. OARSI scoring information has been modified. Please see identified references and OARSI guidelines for further details regarding the scoring system. Information on the staining process we used has been modified. Details regarding slide selection, staining, and imaging have been included. It is difficult to provide full details on software clicks without including commercial language. More detailed demonstration will occur during the video process.
15. Some details moved to introduction and discussion sections. Again, some details regarding software clicks are difficult to describe in full details without using some commercial language of the software product.

16. We have highlighted approximately 2.75 pages of the protocol to be used for filmable content. We will be focusing on the histomorphometric measurements that we describe within the protocol section.
17. We have not reused any figure from any previous publications and thus have not had to obtain explicit copyright permission within our manuscript.
18. Embedded table has been removed from the manuscript and uploaded to the submission portal as an excel file.
19. Discussion section has been revised to include a) critical protocol steps, b) modifications and troubleshooting, c) limitations of the technique, d) significance compared to other current available methods, and e) future applications and developments of the technique.
20. Format for the references has been modified using the JoVE formatting for EndNote.

Replies to Reviewers' Comments:

Reviewer #1:

Major Concerns:
Discussion Lines 331-336: Here you introduce the concept of score repeatability and interobserver reliability, yet no data supporting these statements is presented anywhere in the manuscript. Calculation of relevant statistics is not described in the statistical methods. Can you compare the repeatability and reliability of this evaluation method compared to the OARSI scoring system?
Response: Figure 4 was added to address the topic of inter-observer variability. Additional information was included in the discussion section. Calculation of relevant statistics was included (line 358-366).

Minor Concerns:

Title
As this system was only evaluated in a single preclinical model, the title seems too generalized. Consider altering to more accurately reflect what was done.
Response: Title was modified to reflect specific mouse model used for this protocol. Potential application to other protocols is discussed at the end of the discussion section (line 541).

Protocol
Lines 78-91: The mice used need to be described according to standard reporting protocols, including age, sex, strain, housing, and number used. Why was there not randomization of the treated/sham joints?
Response: Detailed description of mice used for DMM surgery was added to the beginning of the protocol section including all appropriate reporting protocols, lines 97-101.

Lines 103, 114, 117: Please be more specific about the "levels" that were selected. A figure would be most useful to illustrate this, but a more thorough description of the selected anatomical locations would suffice. Were these same levels selected for every mouse? If not,

why not?
Response: Description of level selection was added to protocol section (lines 211-219).

Lines 201-202: This sentence is redundant and does not make sense as written, please revise.
Response: Sentence was modified, no longer the same number line.

Reviewer #2:
Manuscript Summary:
In protocol section there was not information about the anaesthetic protocol used as well as the use of anti-inflammatory, analgesic and antibiotic drugs. In my opinion should be provided information about this because the proper use of an anaesthetic protocol and post-surgery medication would improve the animal protocol as well as the animal welfare.
Response: Detailed description of animal protocol was added and mentioned following NIH and institutional animal care guidelines (lines 97-107).

Sample collection:
- Slides were selected from 3 representative levels of each sample. Please clarify in the text which were considered representative levels.
Response: Description of level selection was added to protocol section (lines 211-219).

OARSI scoring:
- Again it is necessary information about the three representative levels.
Response: Description of level selection was added to protocol section (lines 211-219).

Histomorphometry using OsteoMeasure:
- The lines for cartilage and subchondral bone area measurement were manually drawn or automatically detected by the program?
Response: This was described in the revised manuscript throughout the protocol section.

4.3 Please, explain how the counting function Works, or the parameters to have into account, to differentiate producing and non-producing cells. Describe how you made these discriminations.
Response: Description was added to the protocol section of the manuscript (lines 297-302).

Discussion:
In introduction you explain that other authors tried to make an histomorphometric evaluation of cartilage and subchondral bone parameters. In discussion you may explain why the use of OsteoMeasure software would improve this evaluation respect to other methods.
Response: This was addressed at the end of the discussion section (lines 527-546).

Major concern:

Sample collection:
- Authors used only ketamine for euthanasia? Please provide information about the euthanic

method. If only ketamine for immobilization of animals and perfusion of formaldehyde were used it was a non-valid method for mice euthanasia. In the AVMA Guidelines for the Euthanasia of animals: 2013 Edition (ISBN: 978-1-882691-21-0) explain accepted method for euthanasia. For ketamine says: " These agents are not FDA approved for use as agents of euthanasia. (2) Doses that consistently produce rapid death have not been established for most drugs and species. (3) The cost of the higher doses of agents required to cause death may substantially exceed that of an approved euthanasia agent. " and also "In species for which effective euthanasia doses and routes have been established, overdose of dissociative agent-a-2-adrenergic combinations is an acceptable method of euthanasia" so a combination with xylazine or medetomidine should be done. Also with formaldehyde says "Formaldehyde is an acceptable method of euthanasia for Porifera species. Formaldehyde is acceptable as an adjunctive method of euthanasia for Coelenterates (comb jellies, corals, anemones) and Gastropod molluscs (snails, slugs) only after these animals have been rendered nonresponsive by other methods (eg, magnesium chloride330). Formaldehyde is unacceptable as a first step or adjunctive method of euthanasia for other animal species". Having this in concern, please provide the euthanic protocol used or provide an explanation and the ethical committee approval for the use of this method.

Response: Detailed description of animal protocol was added and includes greater information regarding the euthanic method for this protocol. Ethical committee approval was also noted at the beginning of the revised protocol section.

Thank you again for taking the time to review and edit our work. We look forward to working with the JoVE team for filming the protocol.

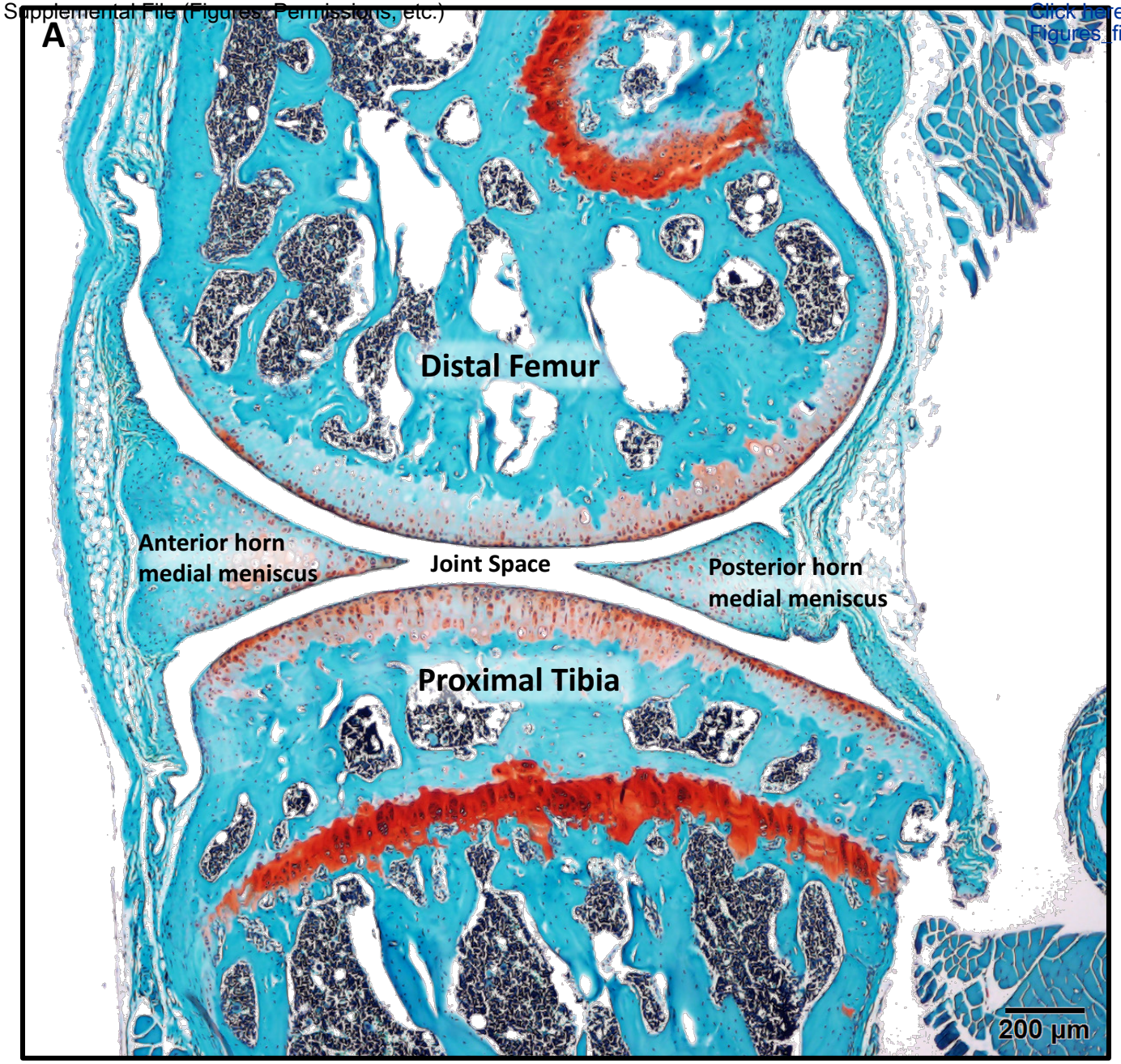

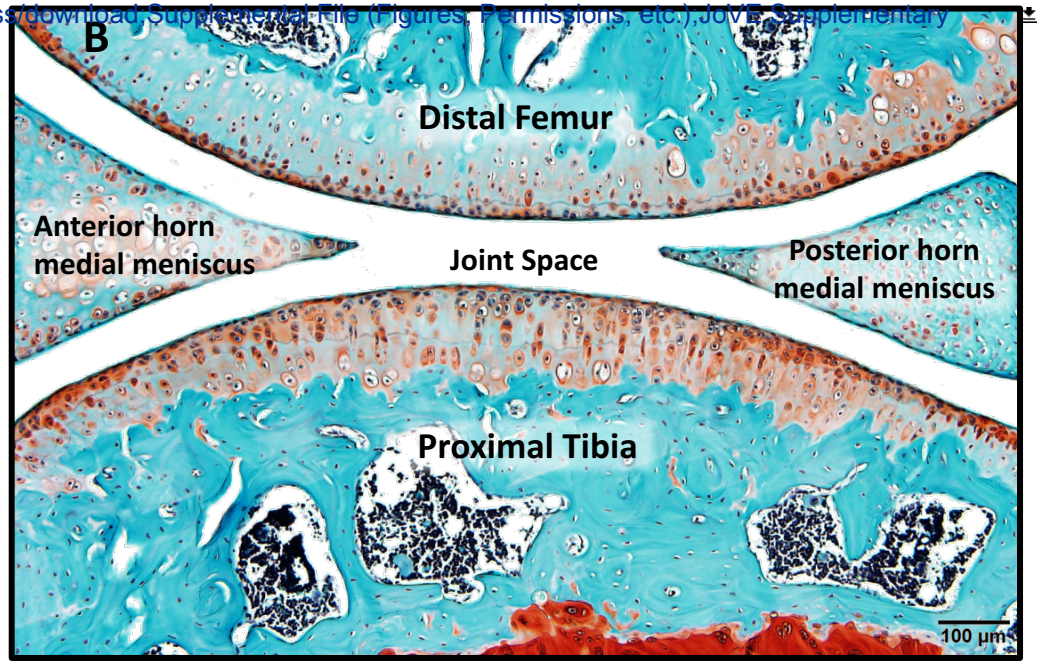

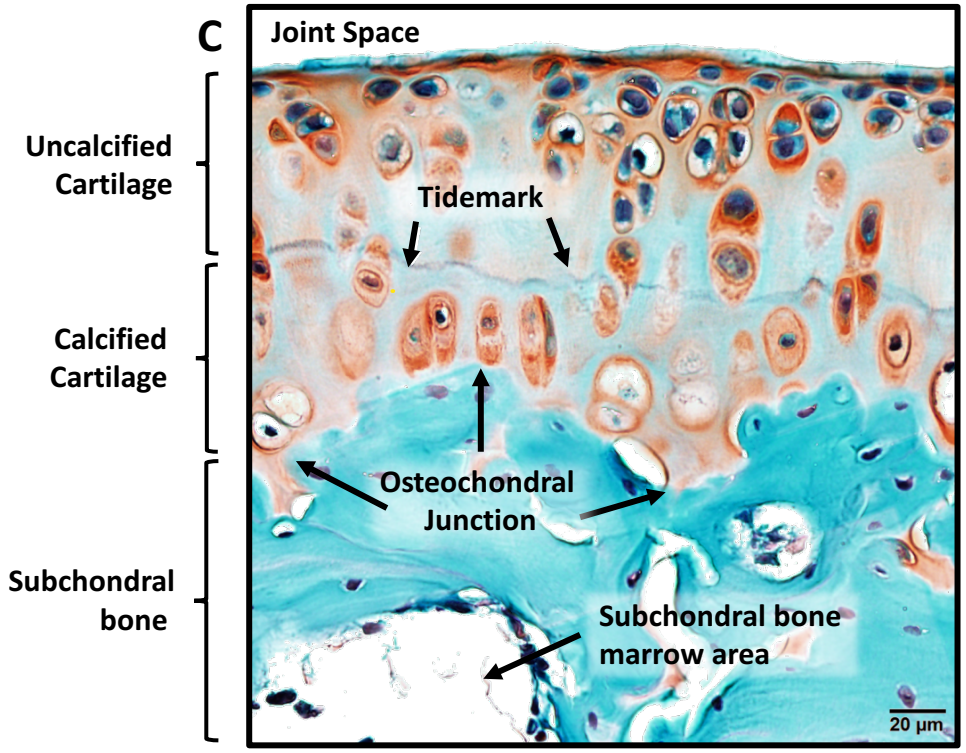

A

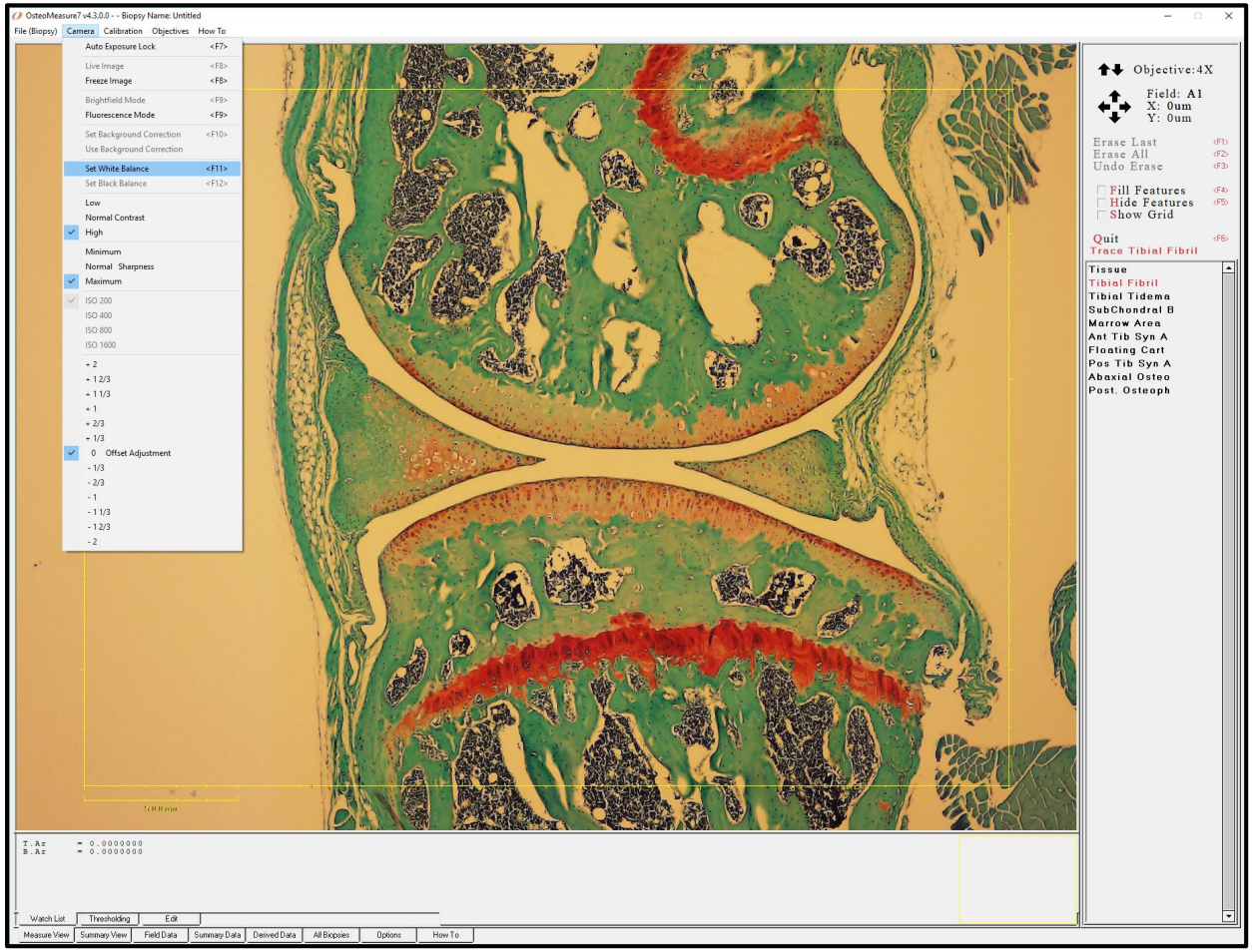
OsteoMeasure7 v4.3.0.0 - - Biopsy Name: Untitled
File (Biopsy) Camera Calibration Objectives How To
Auto Exposure Lock <F7>
Live Image <F8>
Freeze Image <F8>
Brightfield Mode <F9>
Fluorescence Mode <F9>
Set Background Correction <F10>
Use Background Correction
Set White Balance <F11>
Set Black Balance <F12>
Low
Normal Contrast
High
Minimum
Normal Sharpness
Maximum
ISO 200
ISO 400
ISO 800
ISO 1600
+ 2
+ 1 2/3
+ 1 1/3
+ 1
+ 2/3
+ 1/3
0 Offset Adjustment
- 1/3
- 2/3
- 1
- 1 1/3
- 1 2/3
- 2
Objective:4X
Field: A1
X: 0um
Y: 0um
Erase Last <F1>
Erase All <F2>
Undo Erase <F3>
Fill Features <F4>
Hide Features <F5>
Show Grid
Quit <F6>
Trace Tibial Fibril
Tissue
Tibial Fibril
Tibial Tidema
SubChondral B
Marrow Area
Ant Tib Syn A
Floating Cart
Pos Tib Syn A
Abaxial Osteo
Post. Osteoph
T.Ar = 0.0000000
B.Ar = 0.0000000
Watch List
Thresholding
Edit
Measure View
Summary View
Field Data
Summary Data
Derived Data
All Biopsies
Options
How To

B

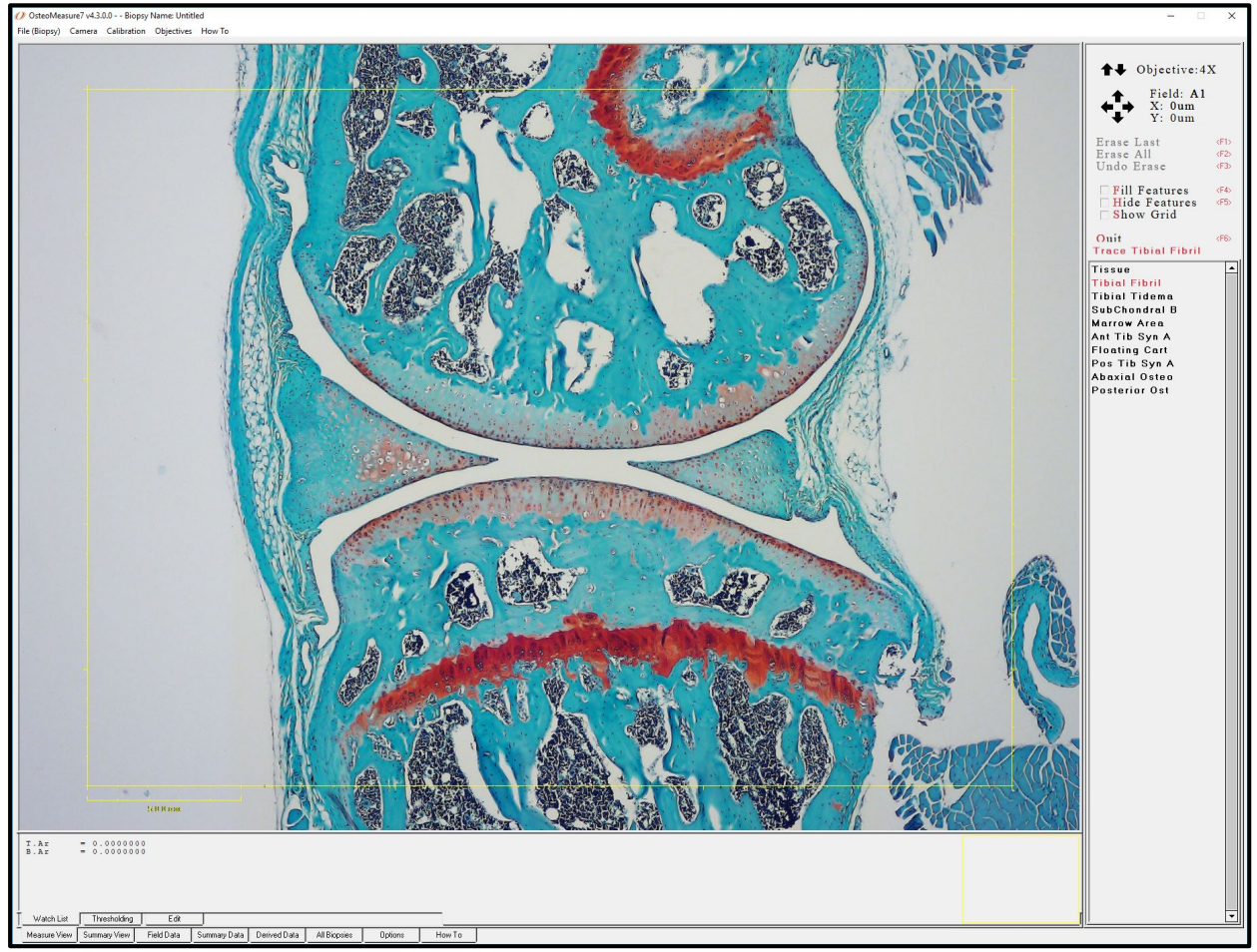
OsteoMeasure7 v4.3.0.0 - - Biopsy Name: Untitled
File (Biopsy) Camera Calibration Objectives How To
Objective:4X
Field: A1
X: 0um
Y: 0um
Erase Last <F1>
Erase All <F2>
Undo Erase <F3>
Fill Features <F4>
Hide Features <F5>
Show Grid
Quit <F6>
Trace Tibial Fibril
Tissue
Tibial Fibril
Tibial Tidema
SubChondral B
Marrow Area
Ant Tib Syn A
Floating Cart
Pos Tib Syn A
Abaxial Osteo
Posterior Ost
T.Ar = 0.0000000
B.Ar = 0.0000000
Watch List
Thresholding
Edit
Measure View
Summary View
Field Data
Summary Data
Derived Data
All Biopsies
Options
How To

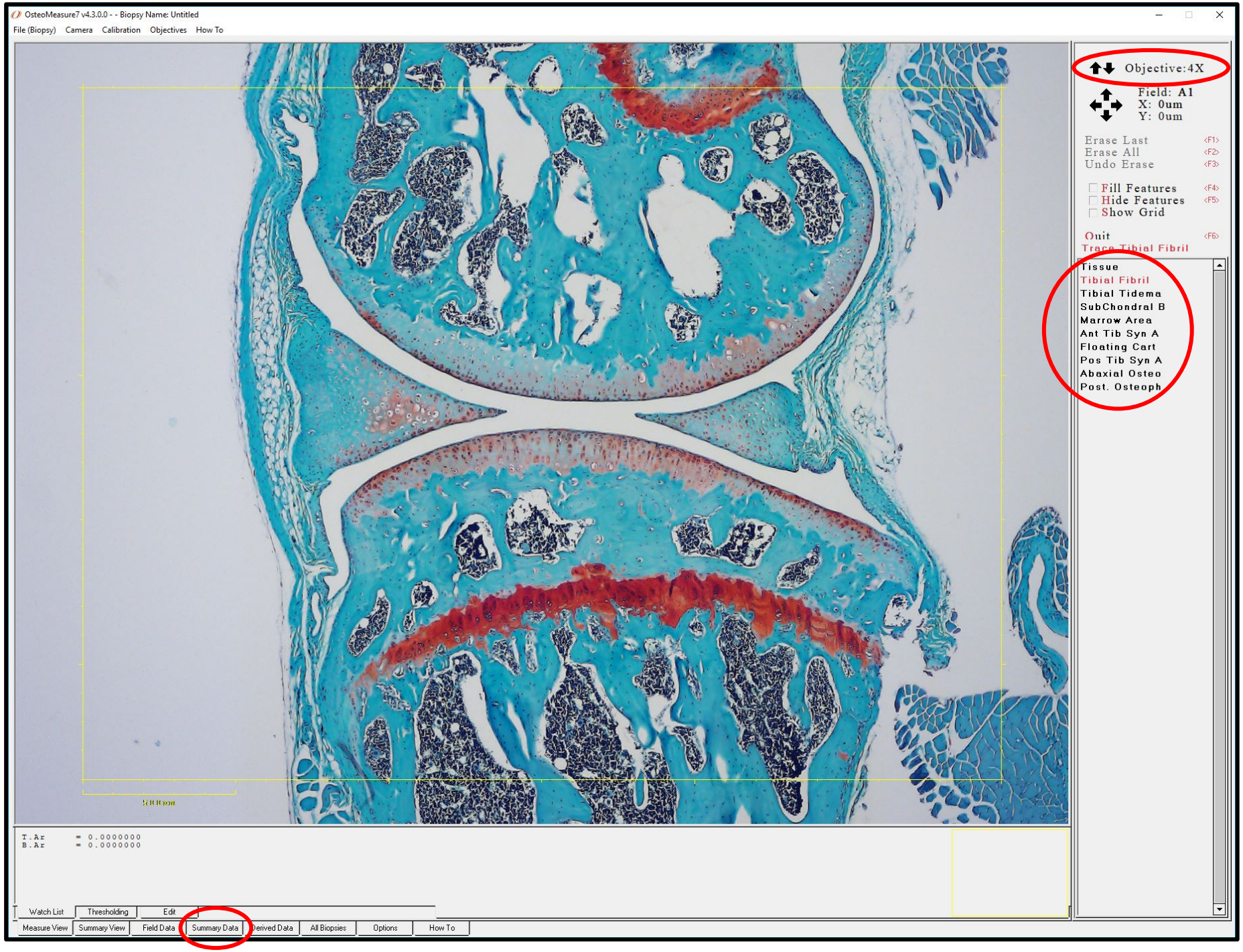
OsteoMeasure7 v4.3.0.0 - - Biopsy Name: Untitled
File (Biopsy)
Camera
Calibration
Objectives
How To
Objective:4X
Field: A1
X: 0um
Y: 0um
Erase Last <F1>
Erase All <F2>
Undo Erase <F3>
Fill Features <F4>
Hide Features <F5>
Show Grid
Quit <F6>
Trace Tibial Fibril
Tissue
Tibial Fibril
Tibial Tidema
SubChondral B
Marrow Area
Ant Tib Syn A
Floating Cart
Pos Tib Syn A
Abaxial Osteo
Post. Osteoph
T.Ar = 0.0000000
B.Ar = 0.0000000
Watch List
Thresholding
Edit
Measure View
Summary View
Field Data
Summary Data
Derived Data
All Biopsies
Options
How To